NASA Technical Memorandum 107494

A General Reversible Hereditary Constitutive Model: Part II—Application to a Titanium Alloy

S.M. Arnold
Lewis Research Center, Cleveland, Ohio

A.F. Saleeb
University of Akron, Akron, Ohio

M.G. Castelli
NYMA, Inc., Brook Park, Ohio

December 1997

The NASA STI Program Office . . . in Profile

Since its founding, NASA has been dedicated to the advancement of aeronautics and space science. The NASA Scientific and Technical Information (STI) Program Office plays a key part in helping NASA maintain this important role.

The NASA STI Program Office is operated by Langley Research Center, the Lead Center for NASA's scientific and technical information. The NASA STI Program Office provides access to the NASA STI Database, the largest collection of aeronautical and space science STI in the world. The Program Office is also NASA's institutional mechanism for disseminating the results of its research and development activities. These results are published by NASA in the NASA STI Report Series, which includes the following report types:

- TECHNICAL PUBLICATION. Reports of completed research or a major significant phase of research that present the results of NASA programs and include extensive data or theoretical analysis. Includes compilations of significant scientific and technical data and information deemed to be of continuing reference value. NASA's counterpart of peer-reviewed formal professional papers but has less stringent limitations on manuscript length and extent of graphic presentations.

- TECHNICAL MEMORANDUM. Scientific and technical findings that are preliminary or of specialized interest, e.g., quick release reports, working papers, and bibliographies that contain minimal annotation. Does not contain extensive analysis.

- CONTRACTOR REPORT. Scientific and technical findings by NASA-sponsored contractors and grantees.

- CONFERENCE PUBLICATION. Collected papers from scientific and technical conferences, symposia, seminars, or other meetings sponsored or cosponsored by NASA.

- SPECIAL PUBLICATION. Scientific, technical, or historical information from NASA programs, projects, and missions, often concerned with subjects having substantial public interest.

- TECHNICAL TRANSLATION. English-language translations of foreign scientific and technical material pertinent to NASA's mission.

Specialized services that complement the STI Program Office's diverse offerings include creating custom thesauri, building customized data bases, organizing and publishing research results . . . even providing videos.

For more information about the NASA STI Program Office, see the following:

- Access the NASA STI Program Home Page at ***http://www.sti.nasa.gov***

- E-mail your question via the Internet to help@sti.nasa.gov

- Fax your question to the NASA Access Help Desk at (301) 621-0134

- Telephone the NASA Access Help Desk at (301) 621-0390

- Write to:
  NASA Access Help Desk
  NASA Center for AeroSpace Information
  800 Elkridge Landing Road
  Linthicum Heights, MD 21090-2934

NASA Technical Memorandum 107494

A General Reversible Hereditary Constitutive Model: Part II—Application to a Titanium Alloy

S.M. Arnold
Lewis Research Center, Cleveland, Ohio

A.F. Saleeb
University of Akron, Akron, Ohio

M.G. Castelli
NYMA, Inc., Brook Park, Ohio

National Aeronautics and
Space Administration

Lewis Research Center

December 1997

Trade names or manufacturers' names are used in this report for identification only. This usage does not constitute an official endorsement, either expressed or implied, by the National Aeronautics and Space Administration.

Available from

NASA Center for Aerospace Information
800 Elkridge Landing Road
Linthicum Heights, MD 21090-2934
Price Code: A03

National Technical Information Service
5287 Port Royal Road
Springfield, VA 22100
Price Code: A03

A General Reversible Hereditary Constitutive Model : Part II Application To A Titanium Alloy

S. M. Arnold
National Aeronautics and Space Administration
Lewis Research Center
Cleveland OH, 44135

A. F. Saleeb*
Department Civil Engineering
University of Akron
Akron, OH 44325

M.G. Castelli
NYMA Inc.
Engineering Services Division
Brook Park, OH 44142

Abstract

Given the mathematical framework and specific viscoelastic model in Part I our primary goal in this second part is focused on model characterization and assessment for the specific titanium alloy, TIMETAL 21S. The model is motivated by experimental evidence suggesting the presence of significant rate/time effects in the so-called quasilinear, reversible, material response range. An explanation of the various experiments performed and their corresponding results are also included. Finally, model correlations and predictions are presented for a wide temperature range.

Keywords: viscoelasticity, hereditary behavior, TIMETAL 21S, nonisothermal, deformation, experimental testing

1 Introduction

In Part I of this paper [1] a general viscoelastoplastic model was discussed, within a potential based framework, in which both the strain (reversible and irreversible) and stress (equilibrium and nonequilibrium) state variables are specifically partitioned. The

*Research funded by NASA Lewis under Grant NAG3-1747.

primary focus there was on the specification of a multiaxial, nonisothermal linear viscoelastic model to describe the reversible strain component wherein the theoretical foundation and numerical implementation of these general descriptions were discussed. A parametric study was then performed, including a number of qualitative response assessments to help identify key factors in the formulation and actual characterization of the specific form of the model. An important conclusion resulting from that study was the importance of assuming each mechanical element's Poisson's ratio to be identical. Three key features resulting from this assumption are the ability to: 1) reduce a multiaxial formulation to that of the classical uniaxial form, 2) easily and uniquely identify a set of two characteristic internal material time clocks, and 3) significantly reduce the required number of material parameters and correspondingly the characterization effort.

The objective of this second part of the paper is to assess the veracity of this viscoelastic model by applying it to a titanium alloy of interest. The specific titanium alloy investigated is **TIMETAL 21S**[1] which was the system previously characterized [[2], [3], [4]]. An outline of the remainder of the paper is as follows: In section 2 we describe the exploratory and characterization experimental program undertaken. In section 3, compact forms summarizing the multiaxial and uniaxial, equal-Poisson's ratio model are stated, followed by the steps taken to characterize (fit) the model in section 4. Lastly, in section 5, we demonstrate the correlation and predictive capability of the model.

2 Viscoelastic Exploratory and Characterization Tests

As previously stated, the material of choice for characterizing the current nonisothermal viscoelastic formulation is the titanium alloy, **TIMETAL 21S**. This alloy was selected due to the considerable attention it has received for use in titanium matrix composites (TMCs) with application toward advanced airframe and engine structures. **TIMETAL 21S** is a β-titanium alloy with a nominal composition of Ti-15Mo-3Nb-3Al-0.2Si (wt. %). The coupon specimens used in this study were taken from "fiberless" panels. The fiberless panels were fabricated by hot isostatic pressing of 0.13mm thick **TIMETAL 21S** foils so as to subject the matrix material to an identical processing history as that seen by the matrix material in the composited form. All specimens were subjected to a pre-test heat treatment, consisting of an 8 hour soak in vacuum at 621°C, to stabilize the β+α microstructure of the **TIMETAL 21S**. For further material, machining, and experimental details see Castelli et al. [5]. All tests addressed are uniaxial experiments, thus implying that the multiaxial material constants are typically generalized from their uniaxial counterparts. This need for generalization is precisely why a consistent multiaxial theory, such as that developed from a potential formulation, is imperative. The available tests for use in characterizing the current nonisothermal equal Poisson's ratio viscoelastic model consist of at least one creep and relaxation test spanning the representative domains in temperature. Very few repeats were performed due to the limited

[1]TIMETAL 21S is a registered trademark of TIMET, Titanium Metals Corporation, Toronto, OH.

amount of available material.

The intent of this section is to provide the reader with the necessary background to understand how the various tests were performed and to motivate and validate some of the key theoretical assumptions made in Part I [1].

2.1 Exploration of Viscoelastic Effects

The first evidence of purely viscoelastic behavior, i.e., the quasilinear reversible regime, in a titanium alloy was observed during the process of characterizing what was originally referred to as the viscoplastic behavior of **TIMETAL 21S**. Specifically, an experimental probing routine was devised to measure the load levels at which the onset of inelastic flow occurred, so as to explicitly distinguish the "elastic" (assumed to be time-independent, reversible) regime from the "viscoplastic" (a time-dependent irreversible) regime. This temperature and rate dependent locus of points defining the onset of inelastic behavior in the context of a multiaxial stress space is commonly known as the "yield" (or in viscoplasticity, the threshold) surface, whose size determining parameter herein, referred to as kappa (κ), is usually determined from uniaxial experiments - see [3] .

The specific probing experiment was defined as follows: At any given temperature and loading rate, a coupon specimen was incrementally loaded to successively larger loads, with an imposed hold period of approximately 1 hour (arbitrary) between each step. During the load hold periods, the material would be carefully monitored for the occurrence of a given arbitrarily established (but sufficiently small) amount of creep strain, say 25 $\mu\varepsilon$[2]. In the event that "no" creep strain was observed, the next load increment was added and the test continued until the criterion was satisfied. When a creep event was observed, the specimen was unloaded and the discrete value of stress at which the creep criterion was satisfied was taken to be the threshold, κ. An additional check on the degree of inelastic strain incurred was then made by measuring the zero-load strain offset subsequent to the unload. In theory, given that the load-up was elastic (reversible), and the creep strain was inelastic (irreversible), the magnitude of the inelastic strain offset subsequent to the elastic unload should match that observed in creep; here is where the problem arose. It was quickly observed that this "additional check" was satisfied only immediately (in time) after the unload. That is, upon complete unloading to zero load and waiting, the specimen exhibited full strain recovery. At this point, it was obvious that our definition for the on-set of inelastic strain (i.e., κ) had to be revisited, and further, that the material was clearly exhibiting time-dependent recoverable (i.e., viscoelastic) behavior.

Having determined that the titanium alloy being examined indeed exhibited viscoelastic behavior, the next step was to establish, in a qualitative sense, the degree to which it occurred and over what range of temperatures was it active. That is, was the viscoelastic behavior trivial in comparison with other viscous behaviors, and secondly, does this behavior disappear at relatively low temperatures? The experimental goal was to make

[2]The term $\mu\varepsilon$ is used throughout to denote micro strain or $1x10^{-6}$ in/in.

a connection with another well established elastic property which exhibited some form of time dependency; here the obvious choice was static[3] stiffness (i.e., Young's Modulus). It is well known that at elevated temperatures, the measurement of material stiffness as obtained through quasi-static mechanical loadings (see ASTM E111) is dependent upon the loading rate. Thus, it was hypothesized that if the fully reversible stress-strain slope (i.e., stiffness) exhibited time dependency at a given temperature, then the material was in fact "viscoelastic" at that temperature. Further, it was assumed that the degree to which the static stiffness was influenced by loading rate was qualitatively indicative of the degree to which viscoelastic effects were non-trivial. This hypothesis was later confirmed to be correct. Figure 1 illustrates the temperature dependent rate sensitivity of the static stiffness for **TIMETAL 21S**. This "elastic" property is given as measured using loading rates over three orders of magnitude and, as can be seen, reveals significant rate effects. The error bars shown designate representative scatter limits found among specimens taken from a given fiberless panel. Below approximately 300 °C, the static stiffness is independent of time. Above this temperature, this material property becomes increasingly rate sensitive to the degree that it can easily vary by more than 100 percent. Similarly, it is at these relatively high temperatures where time-dependent recoverable strains can be quite significant.

Now having qualitatively established the range over which viscoelastic effects were present and the degree to which material behavior was influenced, the next step in the experimental process was to establish a systematic means by which these effects/behaviors could be quantified. Here the appropriate temperature dependent questions were: At what load level does viscoelasticity appear? At what load level does true irreversible behavior occur (i.e., κ)? and, How do we quantify these behaviors? The answers to the first two questions represent the lower and upper bounds, respectively, for the occurrence of purely viscoelastic effects. Below the lower bound, the material behavior is described by time-independent elasticity, within the bounds it is a combination of time -independent and -dependent "elasticity", and above the upper bound (beyond κ) the material exhibits full viscoelastoplastic behavior. The experimental establishment for the lower bound was relatively straight forward, in that the loading step/probing experimental procedure described above could be utilized. Thus as a lower bound, one takes the discrete point where the onset of any time-dependent behavior occurred. This definition is further qualified by verifying that the strains incurred were in fact recoverable (under zero load conditions).

Additional exploratory experiments indicated the conformity of the observed viscoelastic response with certain classical rehological models. Specifically, with a spring in parallel with a simple Maxwell model (see Fig. 4a of Part I), the model suggests that given a constant load, the deformation response will shut down given sufficient time for the dashpot to dissipate to a state of zero-stress equilibrium. Similarly, for a loading condition where a constant deformation is imposed upon the model, the stress relaxation

[3]The use of the term "static" is to distinguish this time-dependent mechanical property from the time-independent "dynamic" stiffness.

behavior will shut down, again, given sufficient time for the dashpot to reach zero-stress equilibrium. The point at which the time-dependent response ceases is some "time-independent" point indicative of the properties of the lone spring, i.e., the thermoelastic limit (see Part I, sec. 5.1).

Conceptually, we could load this system at any rate to a given value of load and the resulting final strain subsequent to a sufficient hold would be identical, as this is dictated by the spring (or the infinite limit stiffness). If the system were loaded infinitely fast, the dashpot would have all of its load yet to dissipate at the initiation of the macro load hold. Hence the time-dependency can be thought of as being "locked-in" during the load-up. Conversely, if the system were loaded infinitely slow, the dashpot would not develop any load and thus, would have no load left to dissipate at the initiation of the "macro" load hold. In this case, the stiffness of the loading is explicitly that of the spring, and further, represents a uniquely time-independent material response. (Note, this same conceptual argument can be posed for the loading case where a fixed macro-deformation is imposed on the model and the time-dependent behavior is measured through macro stress relaxation, as opposed to macro strain creep.) Therefore, these unique material parameters can be explicitly determined only by allowing the viscoelastic response to sufficiently dissipate and thereby obtaining the final stress-strain state.

2.2 Quantification of Viscoelastic Effects

Given the evidence revealed in the exploratory tests, it was clear that the titanium alloy being examined had a regime where reversible time -independent and -dependent effects were active without incurring irreversible behavior. Thus, it was hypothesized that we should be able to load the specimen in this purely viscoelastic regime, allow sufficient time for the viscous deformation behavior to dissipate, and then obtain the "time-independent" stress-strain point dictated by the material. This was precisely the approach taken.

Shown in Fig. 2 is the viscoelastic creep strain behavior at 650 °C presented as a function of time. Here the stress hold was at 0.5 ksi. As can be seen, the creep strain initiates in what would generally be referred to as primary creep behavior. However, instead of entering a mode of secondary (steady state) creep, at approximately 5 hours the creep strain rate goes to zero (i.e., all creep shuts down) and maintains that state for the next several hours of constant loading. Upon unloading to zero load, subsequent to 12 hours of creep, the data clearly reveal that the creep strain is fully recovered in time. The strain value at which the viscoelastic creep shuts down was approximately 140 $\mu\varepsilon$. Thus, if we were able to load the material to 0.5 ksi in an infinitely slow manner, we would have loaded linearly to the stress/strain point of 0.5 ksi/140 $\mu\varepsilon$. (In fact, the data suggests that we would not have to load infinitely slow, but rather we would need a rate less than or equal to $2.8\text{x}10^{-5}$ ksi/s, or $7.8\text{x}10^{-9}$ ε/s). The slope of this line is indicative of the infinite limit stiffness (i.e., time-independent stiffness) of the lone spring within the standard solid model (Fig. 4a, Part I) and is designated as E_s. If

this theoretical concept is correct, then any and all static hold experiments conducted within the material's viscoelastic regime should dissipate to a stress/strain state on this line. The next experiment conducted was a stress relaxation test (i.e., strain hold) which was loaded to 0.8 ksi. This test, as well as the previous are presented in Fig. 3 in the stress/strain space. As can be seen, the final stress relaxation point, where the relaxation process had indeed shut down, coincided with the E_s line (thermoelastic limit) established by the creep test.

Tests such as those described above at 650 °C were also conducted at temperatures of 565, 482, and 300 °C to characterize the viscoelastic response over the temperature range of interest. Within expected bounds of anticipated experimental scatter and variation in material response, without exception, the viscoelastic material response exhibited consistent behavior. This is further illustrated in Fig. 4 where four tests at 565°C, all within the viscoelastic regime, are shown. As can be seen, the creep and stress relaxation termination points of all four tests are well approximated by a single E_s line. Specifically, if upper and lower bound slopes are established by the data (E_{su} and E_{sl}, respectively) the entire range represents a variation of approximately 15% in E_s. Thus, a best-fit line estimating E_s approximates all of the data with an extreme variation of $\pm 7.5\%$. This is considered excellent agreement when examining creep and stress relaxation data.

2.3 Quantification of Viscoplastic Yield

One of the primary goals in characterizing the viscous behavior of this alloy for purposes of deformation modeling was to establish the temperature dependent stress values at which irreversible strains occur (i.e., κ). This was initially referred to as the threshold between elastic and viscoplastic behavior, but it is now more accurately referred to as the transition point from purely reversible (time-independent and time dependent) to reversible plus irreversible behavior. There are several experimental approaches to determining this threshold value, including the one described above where a step-and-hold probing approach was taken to distinguish the point at which time-dependent behavior was observed. This approach is entirely accurate if the material's viscous behavior is exclusively irreversible, that is, the material transitions from time independent elasticity to time-dependent-plasticity without the presence of any viscoelastic behavior. This is clearly not the case for **TIMETAL 21S**.

An alternative approach, is to monotonically load the material to the point where the proportional limit is distinguished. Further, given that the material exhibits a positive strain rate sensitivity, and that we are attempting to establish the earliest possible threshold for the onset of plasticity (irreversibility), it would seem reasonable that the monotonic tests be conducted with a relatively slow loading rate. This is precisely the approach that was taken [4] prior to our distinguishing between reversible and irreversible time dependent behavior. The κ values determined from such monotonic proportional limit tests conducted with a loading rate of 1 $\mu\varepsilon/\text{sec}$ are shown in Fig. 5. The data are presented in the form of upper and lower bound estimates. These bounds were es-

tablished by first visually approximating the proportional limit (a somewhat subjective task), calling that strain value $\varepsilon_{p.l.}$, and then taking the stress values corresponding to $\pm 15\%$ of $\varepsilon_{p.l.}$ as the upper and lower bounds. This method served well to estimate the proportional limit while at the same time providing sufficient flexibility during characterization of the viscoplastic model, by incorporating the subjectivity involved with experimentally determining a discrete explicit deviation from linearity.

The final and current approach established to determine κ is one which purposefully arose out of the viscoelastic characterization tests. The approach is unique in the sense that it allows, for the first time, **an objective, explicit**, experimental measurement of κ. The underlying concept for the experiment is based upon the assumption that the material's viscoelastic response is invariable, even in the presence of viscoplastic behavior. The idea is to load the specimen to a point beyond κ (i.e., well into the irreversible range) and hold that load for a sufficient amount of time, so as to allow all the viscoelastic (time-dependent reversible) response to be fully exhausted. To be safe one must use as a minimum hold time, the time required for the viscoelastic response to shut down as determined from the viscoelastic characterization tests. Subsequent to this hold period where the creep strain is resulting from both time-dependent reversible and irreversible behavior, the specimen is unloaded and given sufficient time to allow for full recovery of the time-dependent reversible strains. From this data, the excess equilibrium stress[4] corresponding to the irreversible portion of the induced strain is calculated ($\sigma_{xe} = \varepsilon^{IR}\mathrm{E}_s$, consequently this stress is strictly zero for purely reversible behavior) and then simply subtracted from the stress level at which the test is performed ($\sigma_{applied}$) to obtain κ ($\kappa = \sigma_{applied} - \sigma_{xe}$). This value effectively represents the upper bound of the viscoelastic regime, and thereby represents the threshold of irreversible behavior. Appropriately, this technique has been termed, **viscoelastic subtraction**. Results from this approach are also shown in Fig. 5. Note that the viscoelastic subtraction technique results in κ values at the upper temperatures which are best approximated by the lower bound proportional limit κ values (determined by monotonic tests conducted with a loading rate of 1 $\mu\varepsilon$/s). This is reasonable and expected given that the ideal monotonic test for determining κ is one which is conducted with an "infinitely" slow strain rate, as this will yield the minimum value for the time-dependent proportional limit. At temperatures where rate-dependency is modest (e.g., 300°C), the κ values obtained via viscoelastic subtraction should be well approximated by the mean values obtained in the proportional limit tests. Here, the monotonic loading test is not significantly affected by loading rate, thus, reducing the difficulty of determining κ to one which is primarily involved with the subjective task of distinguishing the deviation from linearity. With this said, one would conclude that the original estimation of deviation from proportionality was conservative in the lower temperature regime.

[4]The need to calculate the excess equilibrium stress clearly explains why one must allow sufficient time for all the viscoelastic effects to dissipate, i.e., for the non-equilibrium stress (see Part I) to go to zero .

2.4 Concerning Poissons Ratio

A material behavior issue having central impact on the construction (formulation) of the viscoelastic model was that addressing the constancy of Poisson's ratio throughout the viscoelastic regime. Thus, the experimental evaluation of the time-dependent reversible behavior should include a characterization of the temperature and time-dependent behavior of Poisson's ratio. Shown in Fig. 6 are the quasi-static Poisson's ratio ($-\varepsilon^{width}/\varepsilon^{axial}$) values for **TIMETAL 21S**. Note that the material under investigation is "fiberless composite" and it is not uncommon for some mechanical properties to vary by as much as 10 to 20 percent from one panel to the next as a result of anisotropy introduced because of the rolled foils. Thus, in Fig. 6 we see this type of variation within the three panels used for the experiments being discussed.

The second behavioral aspect of Poisson's ratio was related to the constancy of the property during viscoelastic creep/relaxation. Several attempts were made to measure the transverse strain response as a function of creep/relaxation time with only moderate success. The instrumentation device available was not ideally designed to measure this property over extended time periods at elevated temperatures, but was adequate for the quasi-static measurements shown in Fig. 6. With that stated, however, preliminary measurements have indicated that this property remains constant as a function of creep/relaxation time, and this, independent of temperature. Without further experimental evidence to support a non-constant Poisson's ratio in time, utilization of the more complex theoretical framework, discussed in Part I [1], to accommodate such a behavior is considered unwarranted at this time.

3 Multiaxial Nonisothermal Viscoelastic Theory

Here, the multiaxial and uniaxial, three element, equal-Poisson ratio viscoelastic model derived in Part I [1] is restated. As before, the discussion is limited to a case involving small deformations (in which the initial state is assumed to be stress free) and a **linear** viscous element. A Cartesian coordinate reference frame and index notation are utilized (repeated Roman subscripts imply summation).

3.1 Multiaxial Form

The system of first order differential equations representing the three element linear viscoelastic model of Fig. 4a - Part I, can be defined as follows:

$$\dot{e}_{ij} = E^{-1}_{ijkl}\dot{\sigma}^{s}_{kl} + \theta^{E}_{ij}\dot{T} \tag{1}$$

$$\dot{\sigma}^{s}_{kl} = \overline{EM}_{klij}\{M^{-1}_{ijrs}\dot{\sigma}_{rs} + \eta^{-1}_{ijrs}(\sigma_{rs} - \sigma^{s}_{rs}) + \hat{\theta}_{ij}\dot{T}\} \tag{2}$$

where

$$\overline{EM}_{klij} = \{E^{-1}_{klij} + M^{-1}_{klij}\}^{-1}$$

$$\hat{\theta}_{ij} = \frac{\partial M^{-1}_{ijrs}}{\partial T}(\sigma_{rs} - \sigma^s_{rs}) - \frac{\partial E^{-1}_{ijrs}}{\partial T}\sigma^s_{rs} \tag{3}$$

$$\theta^E_{ij} = \left[\frac{\partial E^{-1}_{ijrs}}{\partial T}\sigma^s_{rs} + \frac{\delta_{ij}}{3}\omega_{\tan}\right] \tag{4}$$

and

$$\omega_{\tan} = \omega + \frac{\partial \omega}{\partial T}\Delta T \tag{5}$$

denotes the instantaneous coefficient of thermal expansion.

Now assuming an **isotropic** material, the general form for the isotropic material tensor (in terms of the Young's modulus E and Poisson's ratio, ν) C_{ijkl} representing any given spring or dashpot element is as follows:

$$C_{ijkl} = E \cdot N_{ijkl} = E\{(\frac{\nu}{(1+\nu)(1-2\nu)})\delta_{ij}\delta_{kl} + \frac{1}{(1+\nu)}(\delta_{ik}\delta_{jl} + \delta_{il}\delta_{jk})\} \tag{6}$$

or

$$C^{-1}_{ijkl} = \frac{1}{E} \cdot N^{-1}_{ijkl} = \frac{1}{E}\{-\nu\delta_{ij}\delta_{kl} + \frac{(1+\nu)}{2}(\delta_{ik}\delta_{jl} + \delta_{il}\delta_{jk})\}$$

where one can write the general isotropic stress-strain relations as follows:

$$\sigma_{ij} = C_{ijkl}e_{kl} \tag{7}$$

or

$$e_{ij} = C^{-1}_{ijkl}\sigma_{kl} \tag{8}$$

Utilizing these above relations and assuming that the Poisson's ratios for each element are the same (consequently, the N_{ijkl} for each element are the same) equations (1) through (4) can be rewritten as

$$\dot{e}_{ij} = \frac{1}{E_s}N^{-1}_{ijkl}\dot{\sigma}^s_{kl} + \theta^E_{ij}\dot{T} \tag{9}$$

$$\dot{\sigma}^s_{kl} = \overline{EM}\{\frac{1}{E_m}\dot{\sigma}_{kl} + \frac{1}{E_\eta}(\sigma_{kl} - \sigma^s_{kl}) + \hat{\theta}_{kl}\dot{T}\} \tag{10}$$

where

$$\overline{EM} = \frac{E_s E_m}{(E_s + E_m)} \tag{11}$$

$$\hat{\theta}_{kl} = N_{klrs}\left(\frac{\partial}{\partial T}(\frac{1}{E_m}N^{-1}_{rsmn})(\sigma_{mn} - \sigma^s_{mn}) - \frac{\partial}{\partial T}(\frac{1}{E_s}N^{-1}_{rsmn})\sigma^s_{mn}\right) \tag{12}$$

$$\theta^E_{ij} = \left[\frac{\partial}{\partial T}(\frac{1}{E_s}N^{-1}_{ijrs})\sigma^s_{rs} + \frac{\delta_{ij}}{3}\omega_{\tan}\right] \tag{13}$$

3.2 Uniaxial Simplification

Now if we further restrict ourselves to the purely uniaxial creep loading (e.g., $\sigma_{11} = \sigma^*$ & $\dot{\sigma}_{11} = \frac{\sigma^*}{t_0}$; $\sigma_{22} = \sigma_{33} = \dot{\sigma}_{22} = \dot{\sigma}_{33} = 0$) case given in section 4.1.1 of Part I, the above equations reduce to the following forms:

$$\mathbf{X} = \sigma^*(1 - (\frac{\alpha\rho}{\tau})e^{-\frac{t}{\tau}}) \begin{bmatrix} 1 \\ 0 \\ 0 \end{bmatrix} \tag{14}$$

$$\mathbf{Y} = \frac{\sigma^*}{E_s}(1 - (\frac{\alpha\rho}{\tau})e^{-\frac{t}{\tau}}) \begin{bmatrix} 1 \\ -\nu \\ -\nu \end{bmatrix} \tag{15}$$

where

$$\rho = \frac{E_\eta}{E_m} \tag{16}$$

$$\tau = \frac{E_\eta}{EM} \tag{17}$$

$$\alpha = (\frac{\tau}{\rho} - 1) = \frac{E_m}{E_s} \tag{18}$$

and $\nu = \nu_s = \nu_m = \nu_\eta$. Consequently, only four independent material parameters are required to fully characterize this theory at a given temperature, i.e., E_s,E_m,E_η,ν. This characterization procedure is discussed in the next section. It is important to note that **only** for the very special case of **zero** Poisson's ratio (complete neglection of the stain component interaction) will the above equations reduce to the "classical" standard linear solid model, see e.g., [6]. Also, α must always be greater than or equal to zero as the spring stiffnesses are always positive or zero, thus $\tau > \rho$.

3.3 Characterization

Given the aforementioned equal Poisson's ratio viscoelastic model, the chacterization of the four required material parameters for a particular material is extremely straight forward, provided at least two tests (a creep and relaxation test) within the reversible domain and knowledge of the rate sensitivity of the static moduli or the dynamic moduli (E_o) are available at various temperatures. It is preferable that both longitudinal and transverse extensometry be utilized for data collection, as the availability of the transverse strain measurements allows validation of the assumption of a time-independent effective Poisson's ratio (that is, the equality of the individual mechanical elements' Poisson ratios) for a given material. This assumption is appropriately satisfied for the present titanium alloy **TIMETAL 21S**, as discussed in the previous experimental data section.

TIMETAL 21S		Temperature, ° C				
Constants	**Units**	**25**	**300**	**482**	**565**	**650**
E_s	Msi	16.5	15.2	11.9	8.1	3.4
E_m	Msi	0	0.35	2.0	5.1	9.0
E_η	Msi sec	—	1,747.6	8,746.8	16,051.2	16,651.2
ρ	sec	—	4993.2	4373.3	3147.3	1850.1
τ	sec	—	5108.4	5108.4	5128.9	6747.5
ν	—	0.33	0.34	0.36	0.365	0.375

Table 1: Nonisothermal material parameters for Timetal 21S.

Given creep and relaxation test results at various temperatures, the following five step procedure should be followed to obtain the required model parameters. First the infinite elastic stiffness, E_s, is directly obtainable from the stress versus strain plot at each available temperature by drawing a line through the end points of both the creep and relaxation data, as shown in Fig. 3. Second, given the dynamic (instantaneous) modulus, E_o, the maxwell spring stiffness, E_m, can be indirectly obtained form the following expression:

$$E_m = E_o - E_s$$

Note if the dynamic modulus is not readily available, one can substitute in for E_o the stiffness associated with the fastest rate of loading available. This later approach was used here as an initial guess for E_o. Third, given a plot of the reversible creep strain versus time information the internal clock parameter, τ, defined to be the characteristic creep time can be determined directly. Since from our previous parametric study results in Part I [1], τ is equal to one seventh of the time to saturation of the creep response (i.e., when the creep strain rate is zero). Now given the two spring stiffnesses, E_s and E_m, and the characteristic creep time, the fourth step is to indirectly calculate the viscous stiffness, E_η, using the expression

$$E_\eta = \frac{\tau E_m}{(1 + \frac{E_m}{E_s})}$$

which comes from equations (17) and (11). The fifth and final step is to determine the temperature dependent Poisson's ratio to be used. Again, this is directly obtainable from the experimental data given the transverse response histories at the temperature of interest. Note as E_m and E_η, were both indirectly obtained, they were considered to be initial estimates only. With some slight refinements being made subsequently to better correlate with the given relaxation data. The resulting optimized viscoelastic material parameter set for **TIMETAL 21S** is given in Table 1.

Temperature, ° C	σmax (ksi)			$e$max ($\mu\epsilon$)		
–	Exp	Corr	% error	Exp	Corr	% error
650	0.551	0.51	7.4	159.5	149.94	6.0
565	1.777	1.73	2.6	211.6	213..58	-0.9
482	7.069	7.0	0.97	590.7	588.2	0.4
300	70.108	70.	0.15	4643.	4613.	0.6

Table 2: Maximum values used for normalization of data in Fig. 7.

Temperature, ° C	σmax (ksi)			$e$max ($\mu\epsilon$)		
–	Exp	Corr	% error	Exp	Corr	% error
650	0.805	0.77	4.3	66.47	64.516	2.9
565	1.682	1.68	0.2	129.1	127.27	1.4
482	7.212	7.1	1.5	509.9	510.8	0.4
300	73.209	73.	0.28	4736.	4702.	0.72

Table 3: Maximum values used for normalization of data in Fig. 8.

4 Results

4.1 Correlations

Given the full multiaxial, nonisothermal, viscoelastic representation of equations (9) and (10), and the material parameters in Table 1 the creep and relaxation correlations shown in Figs. 7 and 8, respectively, can be obtained. The ability of the model to fit the experimental data is very good, particularly when one considers the wide temperature range over which the model is being correlated. A remark with respect to the normalization of the data within these figures is in order; namely, each stress versus strain, strain versus time (in the case of creep) and stress versus time (in the case of relaxation) response curve has been normalized with respect to its maximum value, see Tables 2 and 3 respectively. Consequently, all temperatures can be represented on a single figure and one can immediately see the portion of the total reversible strain (or stress) that is time dependent. For example in Fig. 7a, we see that at 650 °C - 76% of the total strain is time-dependent, while at 565 - 40%, at 482 - 18%, and at 300 °C - only 2% of the total strain is time-dependent. This clearly substantiates the hypothesis put forth in Part I regarding the partitioning of the reversible strain into a time independent and time dependent region. Note that for this material it appears that the purely time dependent reversible domain would not begin until one reached a temperature much higher than 650 °C, see Fig. 3c, Part I. Also, from Tables 2 and 3 it is clear that the correlation was accomplished with less than an 8% maximum error at any given temperature examined.

Stress Rate (ksi/sec)	T= 565 °C	T = 482 °C
5	13.199	13.899
0.5	13.197	13.896
0.05	13.172	13.863
0.005	12.936	13.570
0.0005	11.288	12.435
0.00005	8.591	12.000

Table 4: Rate Dependence of the Effective Stiffness (Msi), see Figs.10 and 11 .

4.2 Predictions

4.2.1 Creep and Relaxation

Subsequent to characterization, the model was then tested by performing a creep and relaxation test at stress levels of 0.6 and 0.8 ksi , respectively, at 565 °C. The model predictions and experimental results are illustrated in Fig. 9, where in Fig. 9a the normalized stress-strain response histories are illustrated and in Fig. 9b the normalized strain-time creep and stress-time relaxation response histories are given for the 565 °C conditions. Clearly, the predictions are in very good agreement with the experimental results. Once again the maximum values are used in the normalization procedure and are given in the figure. Furthermore, although the present viscoelastic model is fully multiaxial, the transverse response histories associated with each temperature are not illustrated as they would amount to nothing more than reducing the longitudinal response by the associated Poisson's ratio at each temperature.

4.2.2 Rate Dependence

Finally, so as to demonstrate the rate dependent nature of the present model, two creep tests - one at 1.7 ksi (565 °C) the other at 7.0 ksi (482 °C) - were repeated with load rates ranging from $5x10^{-5}$ to 5 ksi/sec. Table 4 list the change in effective load-up modulus as a function of applied loading rate for each temperature, whereas Figs. 10 and 11 show the corresponding stress versus strain histories as functions of loading rate. Note that as the loading rate is decreased the stress-strain response tends toward the thermoelastic limit response as it must, yet for all practical purposes above a loading rate of 0.05 ksi/sec the load-up response is basically rate insensitive. This disagrees with the experimental results presented earlier in Fig. 1, as the experimentally obtained stiffness values are indeed rate sensitive within this higher loading rate regime. Consequently, if capturing this higher rate dependence regime is essential to the application being addressed, one would need to generalize the kernel function as outlined in section 5.2 of Part I of this report (see for example, the discrete relaxation spectrum as in equation (87) of said section).

5 Conclusions

In this paper we have describe the exploratory and characterization experiments performed to investigate and demonstrate the various hypotheses discussed in Part I of this paper. Here we have actually correlated, with minimal effort, the specialized multiaxial, equal Poisson's ratio, model (with a single relaxation spectrum) using only a single creep and relaxation test at each temperature. The ability of the model to correlate and predict the corresponding experimental values was shown to be very good for the temperature range of interest. However, it was shown that although the present model does possess loading rate sensitivity, this sensitivity exists in the lower portion of the spectrum (slower loading rate regime) instead of the upper. This is understandable since here we have used only a single exponential term (i.e., Maxwell element) and it was fit to respond to the long term transient response domain. As discussed in Part I, future work will address the incorporation of additional mechanical elements allowing the relaxation spectrum to be broadeded, and in turn, allowing the entire load spectrum to be spanned. Such an extension should be particularly useful with polymer-based material systems.

References

[1] Saleeb, A.F. and Arnold, S.M.: A General Reversible Hereditary Constitutive Model: Part I: Theoretical Developments, submitted to Int. J. Solids and Structures, or NASA TM-107493, 1997.

[2] Arnold, S.M.; and Saleeb, A.F.: On the Thermodynamic Framework of Generalized Coupled Thermoelastic Viscoplastic - Damage Modeling. , Int. Jnl. Plasticity, Vol. 10, No. 3, 1994, pp. 263-278, or NASA TM-105349, 1991.

[3] Arnold, S.M.; Saleeb, A.F., and Castelli, M.G.: A Fully Associative, Nonlinear Kinematic, Unified Viscoplastic Model for Titanium Based Matrices, *Life Prediction Methodology for Titanium Matrix Composites*, ASTM STP 1253, W.S. Johnson, J.M. Larsen, and B.N. Cox, Eds., 1996, or NASA TM-106609, 1994.

[4] Arnold, S.M.; Saleeb, A.F., and Castelli, M.G.: A Fully Associative,Nonisothermal, Nonlinear Kinematic, Unified Viscoplastic Model for Titanium Based Matrices, *Thermomechanical Fatigue Behavior of Materials: Second Volume,* ASTM STP 1263, M.J. Verrilli and M.G. Castelli, Eds., Philadelphia,1995, or NASA TM-106926, 1994

[5] Castelli, M.G., Arnold, S.M., and Saleeb, A.F.:Specialized Deformation Tests for the Characterization of a Viscoplastic Model: Application to a Titanium Alloy, NASA TM-106268, 1995.

[6] Christensen, R., *Theory of Viscoelasticity*, Academic Press, New York, 1971.

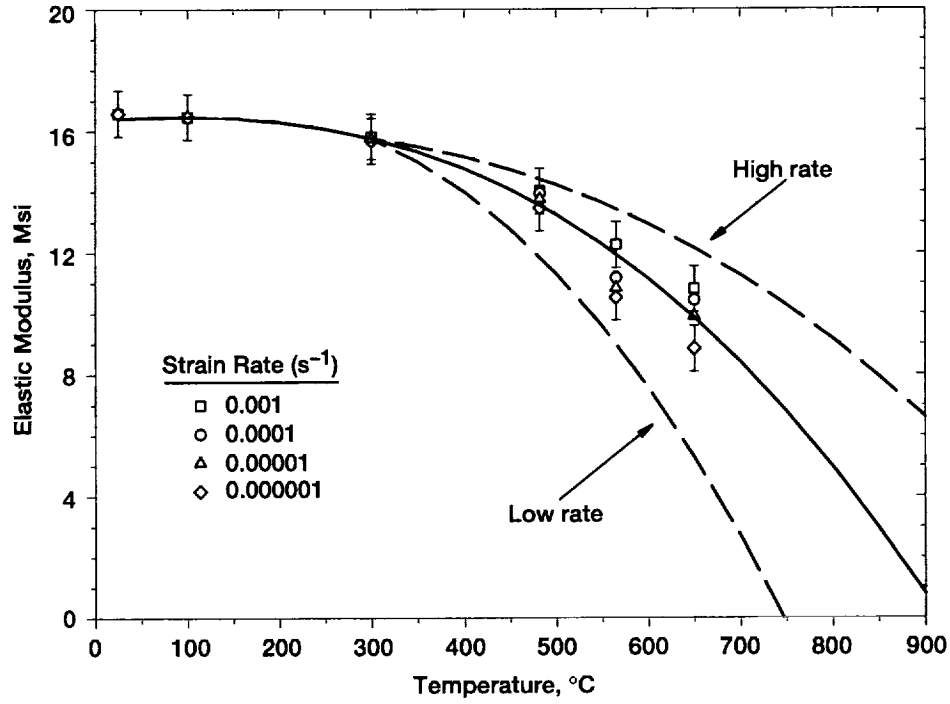

Figure 1.—Rate dependent stiffness.

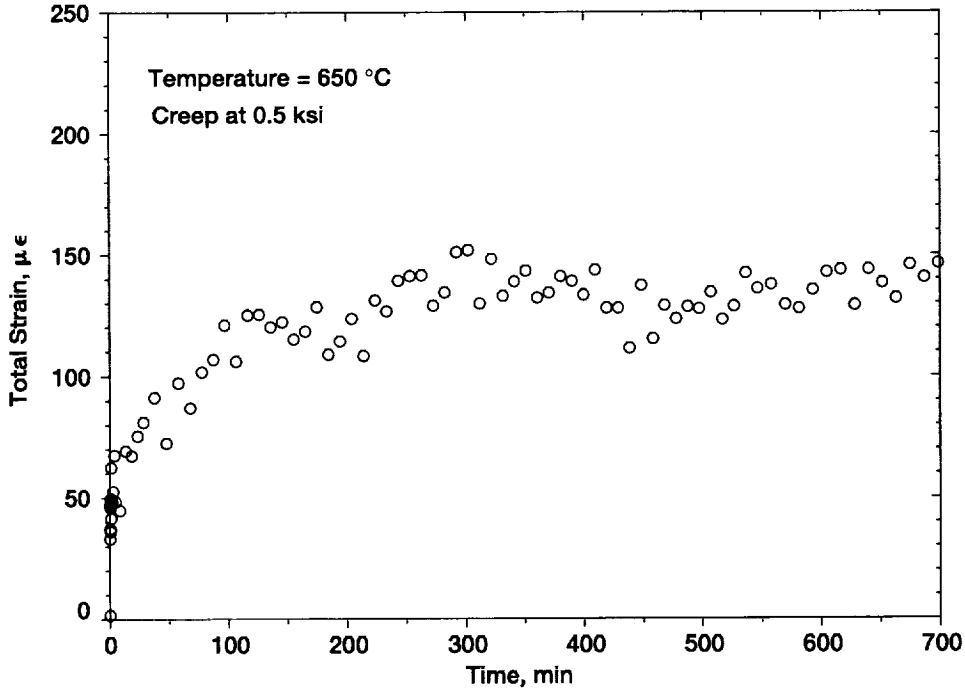

Figure 2.—Viscoelastic creep at 0.5 ksi and 650 °C, (creep strain versus time).

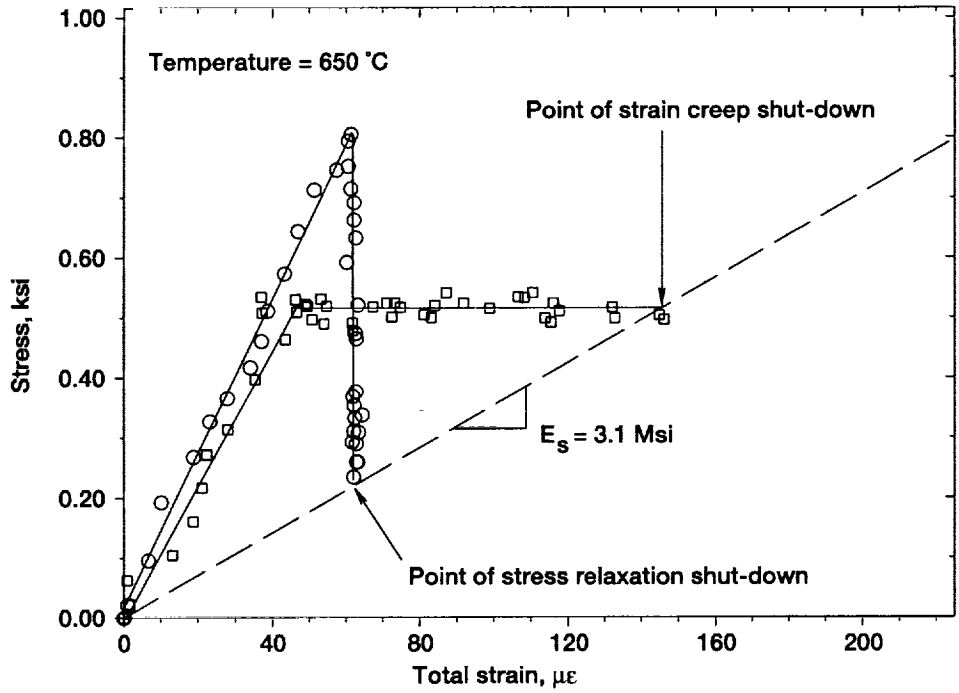

Figure 3.—Viscoelastic creep and stress relaxation at 650 °C, (stress versus strain).

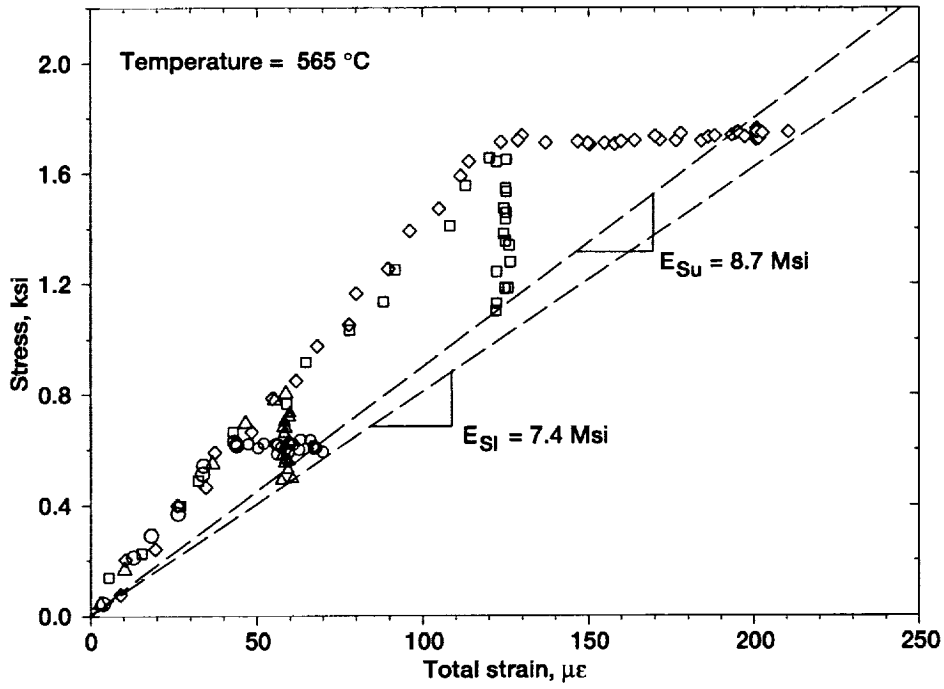

Figure 4.—Viscoelastic creep and stress relaxation at 565 °C, (stress versus strain).

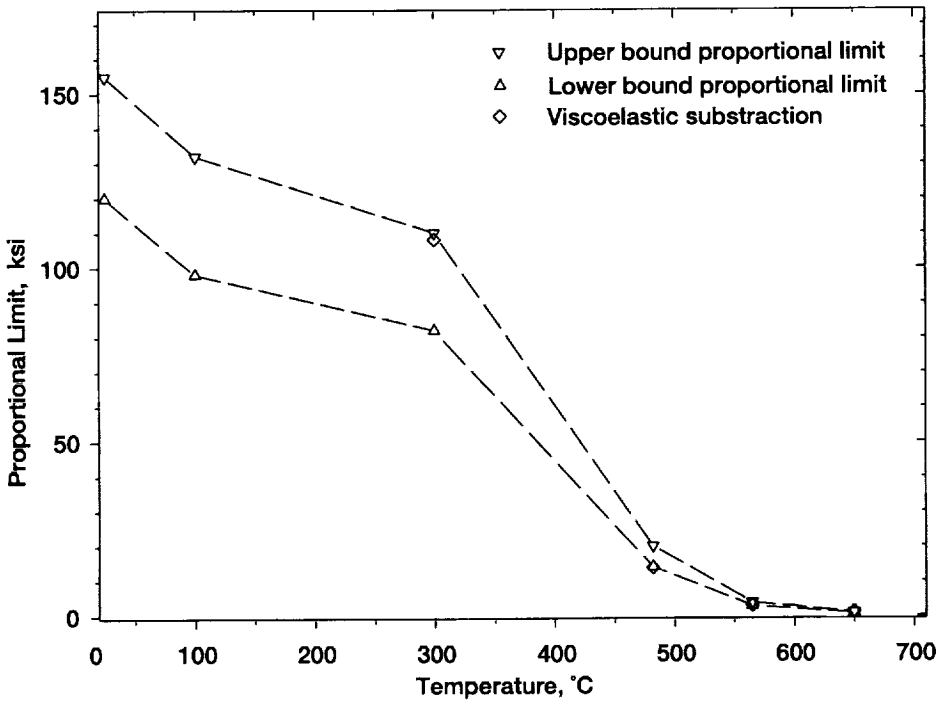

Figure 5.—Kappa as determined from proportional limit and viscoelastic subtraction.

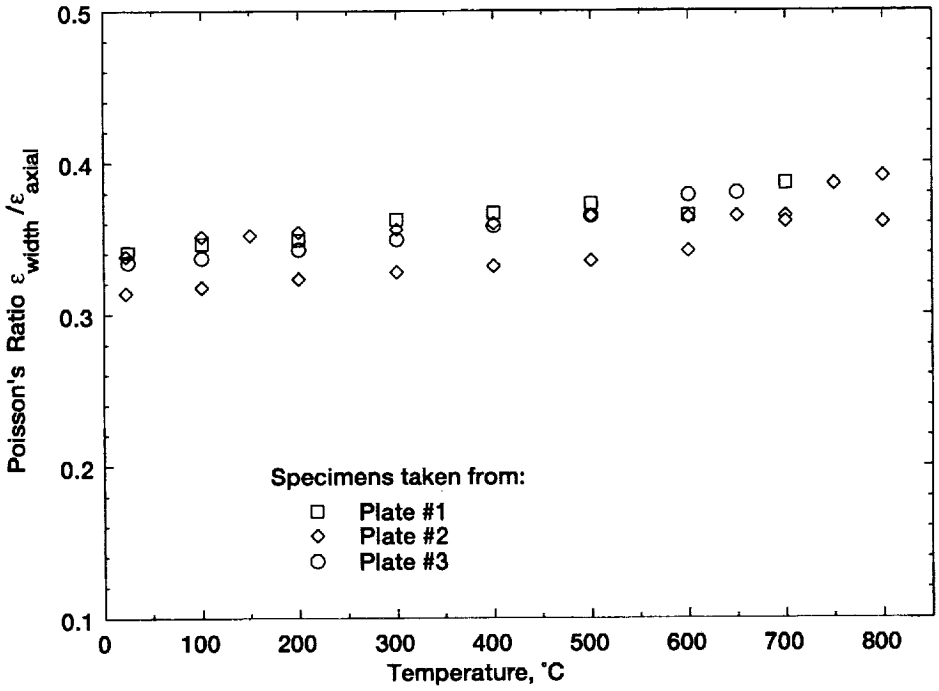

Figure 6.—Poisson's ratio as a function of temperature.

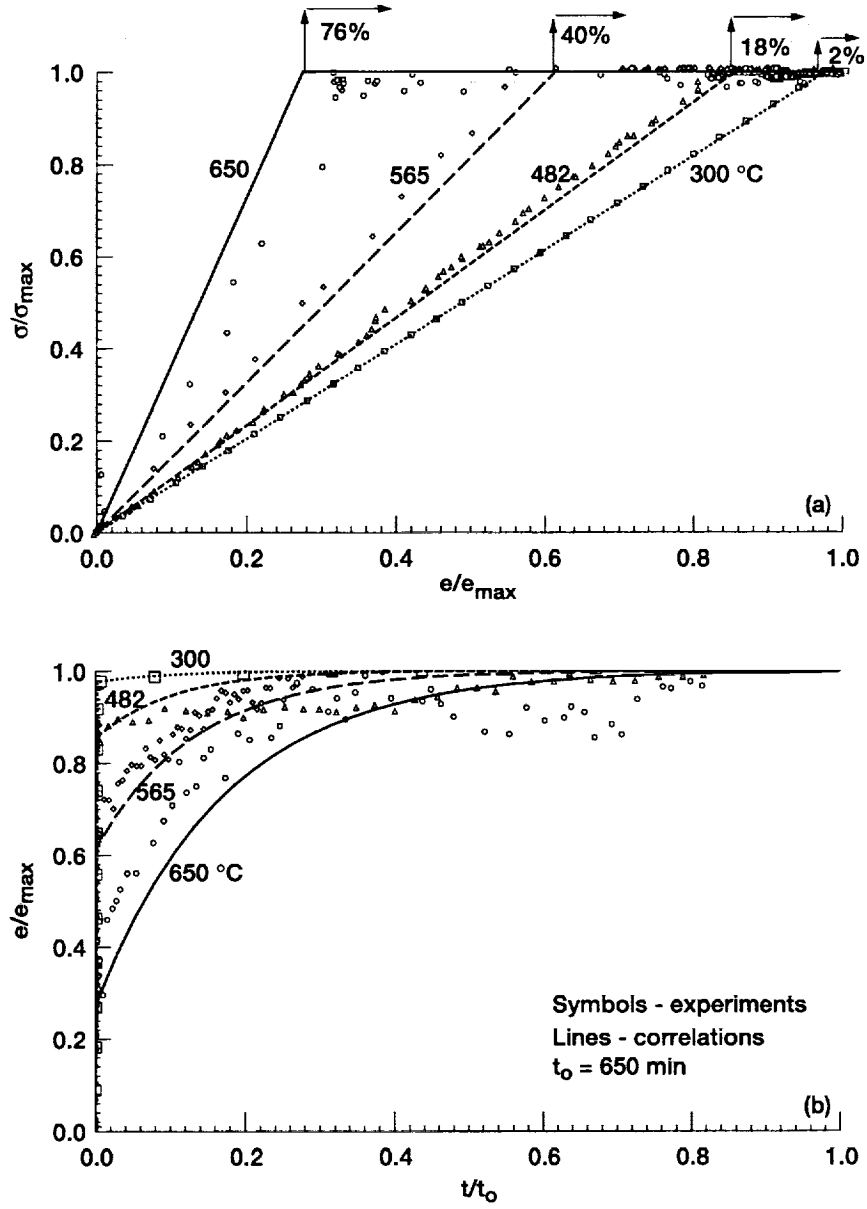

Figure 7.—Nonisothermal viscoelastic creep correlations with experiments.

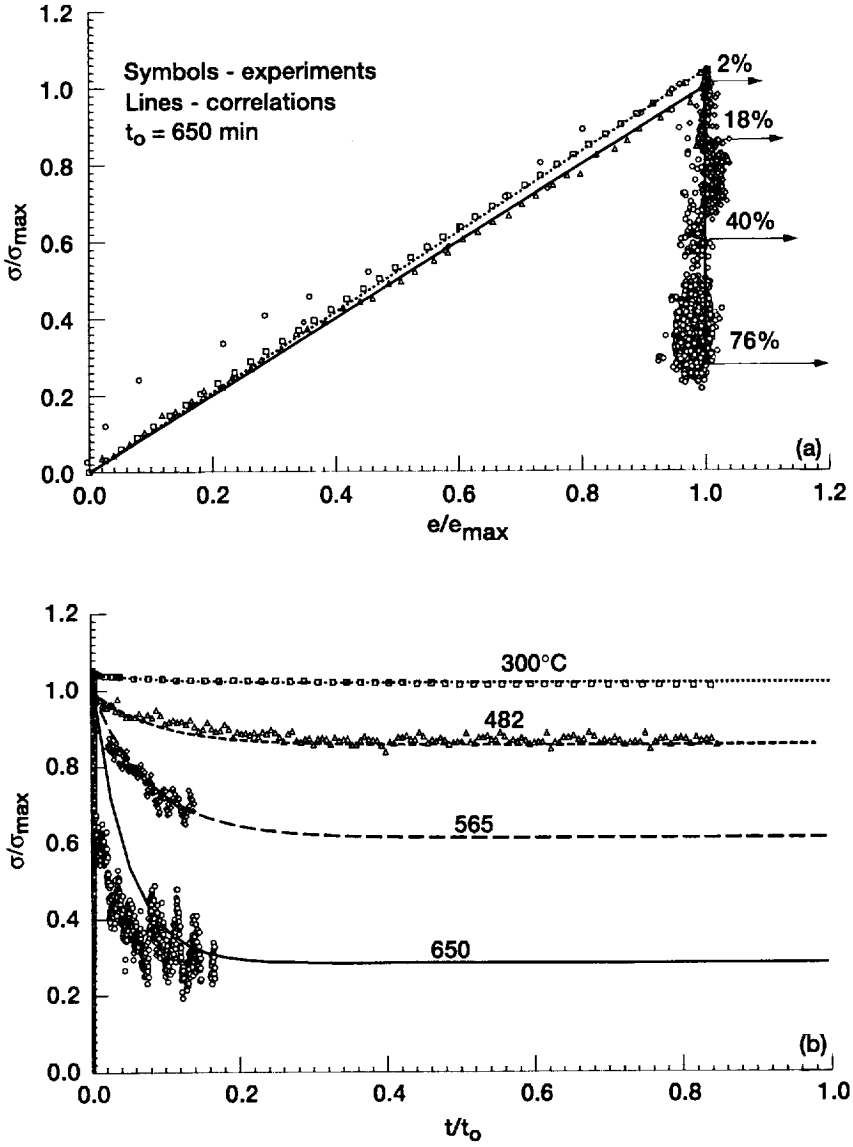

Figure 8.—Nonisothermal viscoelastic relaxation correlations with experiments.

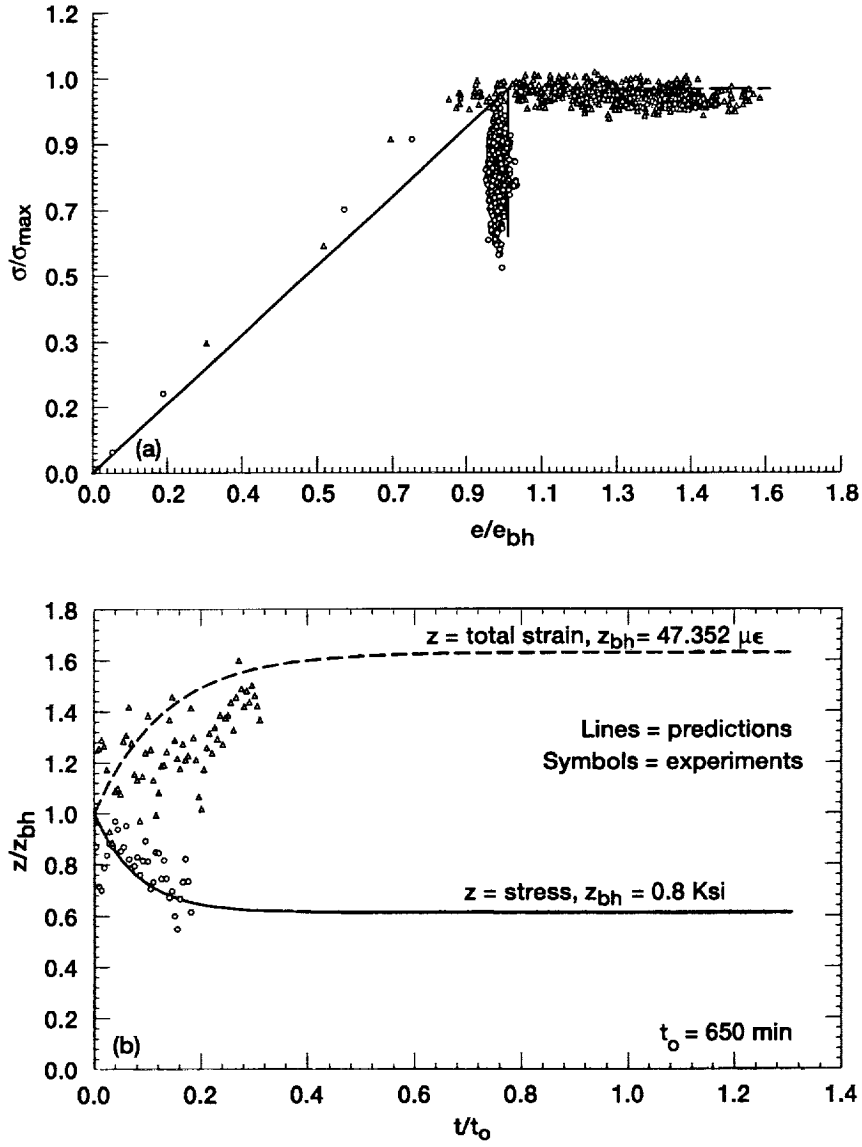

Figure 9.—Pediction of creep and relaxation at 565 °C.

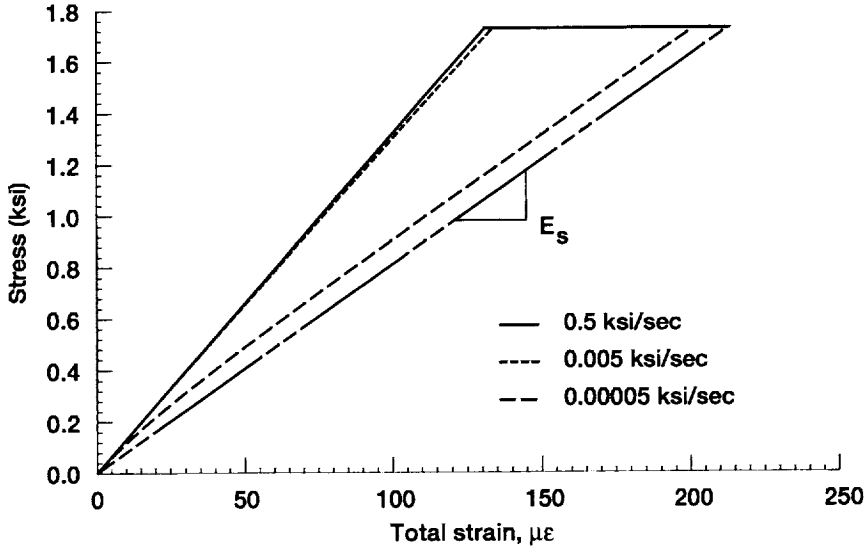

Figure 10.—Effect of loading rate on the creep response at 565 °C.

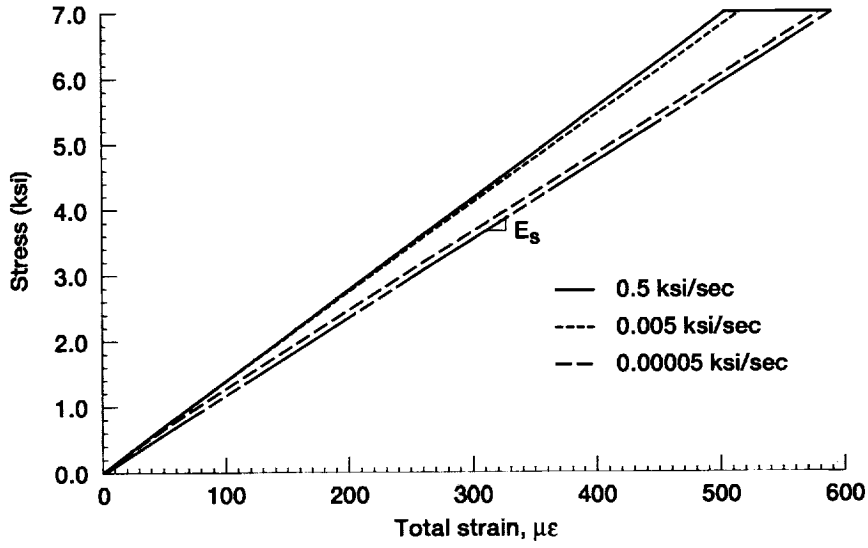

Figure 11.—Effect of loading rate on the creep response at 482 °C.

REPORT DOCUMENTATION PAGE

Form Approved
OMB No. 0704-0188

1. AGENCY USE ONLY (*Leave blank*)	2. REPORT DATE	3. REPORT TYPE AND DATES COVERED
	December 1997	Technical Memorandum

4. TITLE AND SUBTITLE

A General Reversible Hereditary Constitutive Model:
Part II—Application to a Titanium Alloy

5. FUNDING NUMBERS

WU-523-21-13-00

6. AUTHOR(S)

S.M. Arnold, A.F. Saleeb, and M.G. Castelli

7. PERFORMING ORGANIZATION NAME(S) AND ADDRESS(ES)

National Aeronautics and Space Administration
Lewis Research Center
Cleveland, Ohio 44135-3191

8. PERFORMING ORGANIZATION REPORT NUMBER

E-10792

9. SPONSORING/MONITORING AGENCY NAME(S) AND ADDRESS(ES)

National Aeronautics and Space Administration
Washington, DC 20546-0001

10. SPONSORING/MONITORING AGENCY REPORT NUMBER

NASA TM-107494

11. SUPPLEMENTARY NOTES

S.M. Arnold, NASA Lewis Research Center; A.F. Saleeb, University of Akron, Department of Civil Engineering, Akron, Ohio 44325; and M.G. Castelli, NYMA, Inc., Brook Park, Ohio 44142 (work performed under NASA Contract NAS3-27186). Responsible person, S.M. Arnold, organization code 5920, (216) 433-3334.

12a. DISTRIBUTION/AVAILABILITY STATEMENT

Unclassified - Unlimited
Subject Category: 39 Distribution: Nonstandard

This publication is available from the NASA Center for AeroSpace Information, (301) 621-0390.

12b. DISTRIBUTION CODE

13. ABSTRACT (***Maximum 200 words***)

Given the mathematical framework and specific viscoelastic model in Part I our primary goal in this second part is focused on model characterization and assessment for the specific titanium alloy, TIMETAL 21S. The model is motivated by experimental evidence suggesting the presence of significant rate/time effects in the so-called quasilinear, reversible, material response range. An explanation of the various experiments performed and their corresponding results are also included. Finally, model correlations and predictions are presented for a wide temperature range.

14. SUBJECT TERMS

Viscoelastic; Hereditary behavior; Nonisothermal; Deformation; Experimental testing

15. NUMBER OF PAGES

27

16. PRICE CODE

A03

17. SECURITY CLASSIFICATION OF REPORT	18. SECURITY CLASSIFICATION OF THIS PAGE	19. SECURITY CLASSIFICATION OF ABSTRACT	20. LIMITATION OF ABSTRACT
Unclassified	Unclassified	Unclassified	